

WSRC-TR--92-358

DE93 005071

NRTSC
Nuclear Reactor Technology
and Scientific Computations

WSRC-TR-92-358
Task 92-068-1

KEYWORDS:

K-14
Mark 22
Depletion
Axial Flux Shape
GLASS
GRIMHX
Xenon Worth
Initial Critical


Retention-Permanent

**GRIMHX Predictions of Axial Power Shapes and
Xenon Worth with 3-D Depletion Modeling (U)**

By

ROBERT L. FROST
CHRISTA BOMAN
KEYES A. NIEMER

ISSUED: JULY 1992


C.E. Apperson 9-14-92
Reviewing Official


C.E. Apperson 9-14-92
Authorized Derivative Classifier

SRL SAVANNAH RIVER LABORATORY, AIKEN, SC 29808
Westinghouse Savannah River Company
Prepared for the U. S. Department of Energy under Contract
DE-AC09-86SR18035

MASTER

ds
DISTRIBUTION OF THIS DOCUMENT IS UNLIMITED

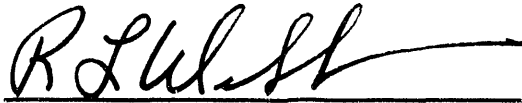
Document: WSRC-TR-92-358

Title: GRIMHX Predictions of Axial Power Shapes
and Xenon Worth with 3-D Depletion
Modeling (U)

Task Number: 92-068-1

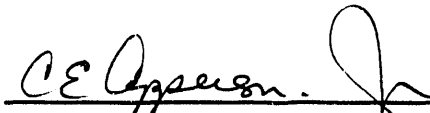
Task Title: Physics Calculations in Support of K-14
Start-Up.

APPROVALS



R.L. Webb, Technical Reviewer

Date: 8/20/92



C. E. Apperson, Manager
Reactor Physics Group

Date: 9-18-92



M.R. Buckner, Manager
Scientific Computations Section

Date: 9/27/92



INTRODUCTION

The extensive number of reactivity tests and power shape measurements that have been an integral part of the K-reactor start-up testing plan have provided the Applied Physics Group a wealth of new data to benchmark physics codes. This data has been obtained under nearly ideal conditions with high quality assurance standards, unlike the limited amount of data available from past operations. Much of this data will be used in benchmarking GRIMHX (Ref. 1). The ability of GRIMHX to accurately predict axial flux and power shapes, given an observed control rod position, has been questioned. This is an important concern since GRIMHX is the 3-D diffusion theory code employed at SRS for reactivity analysis and flux and power distribution calculations. One problem has been finding data appropriate for a comparison. Since GRIMHX does not have a depletion capability, the best reactor data for comparison against GRIMHX power shapes should be obtained at Beginning-of-Cycle (BOC), preferably at zero power (so there are no fission products). Unfortunately, the Axial Power Monitor Rods from which axial power shapes are inferred are not operable at zero power, and are less accurate at low powers than high powers (Ref. 2). These rods are actually gamma thermometers that work by detecting heat deposited from gamma rays within the instrument (under most conditions the gamma ray deposited power is directly proportional to fission power). It follows that meaningful axial power data can only be obtained when the reactor is at power.

The accuracy of GRIMHX axial power shape modeling was questioned recently after completion of Reactor Startup Procedure 90-007-12. This procedure required operators to move all partial rods in gang 1 from 800 to 850 veeder units. The test was performed at a reactor power of approximately 116 MW. Predictions based on GRIMHX indicated a reactivity decrease should occur when the partial rods were inserted, requiring full rods to be withdrawn to compensate. Instead, a reactivity increase was obtained, requiring operators to insert full rods to maintain power at 116 MW. (It should be noted that Reactor Operations personnel determined prior to execution of



**GRIMHX Predictions of Axial Power Shapes and
Xenon Worth with 3-D Depletion Modeling**

the procedure that the reactivity addition would be positive, not negative as had been predicted by calculation. Their determination was based on observed axial power shapes.) This test showed that the GRIMHX predicted axial power shape was quite different from the one present in the reactor.

Acknowledging the importance of being able to accurately predict the axial power shape, the Applied Physics Group is analyzing several possible causes of the inaccurate shape currently predicted. These are:

- 1. Axial xenon build-in.** Even though the reactor was operating at low power for a short period of time, xenon was present, and its concentration was a function of the axial and radial exposure history. This was not accounted for in the original GRIMHX calculations.
- 2. Errors in the GRIMHX coding and/or methodology.** Although this seems unlikely after years of use and testing of the code, the decision was made to compare GRIMHX to the DIF3D and MCNP models of the RSP 90-007-12 test. In addition, an effort was made to provide a transport theory solution to the axial power shape.
- 3. Axial Geometry Modeling.** An in depth study of the actual axial dimensions and concentrations of the fuel and target tubes, as well as the endfittings and control rods, was begun.

This paper reports on the investigation of the first item listed above. The second and third items will be the subject of separate reports by other authors.

A second concern raised around the time of the partial rod insertion test was the prediction of xenon reactivity worth. The predicted value was only 70% of the "observed" value. The technical basis for finding the predicted value seems firm; however, the "observed" value is based on GRIMHX-produced rod worth curves that do not account for fission products. In addition, these curves may suffer from the same inaccurate axial flux shape prediction as discussed



above. The xenon reactivity worth issue has been investigated and is discussed in section 2 of this paper.

Finally, three sets of initial critical full rod positions, corresponding to double partial rods at 700, 800 and 950 veeder units, respectively, have been analyzed. Initial calculations were cause for concern since the value of k-effective calculated with GRIMHX for the three critical states varied by over 600 pcm. Analysis has been performed to lower the discrepancy to only 136 pcm.

SUMMARY

This section summarizes various findings relating to axial power shapes. Specific details on results obtained by other task teams within APG will be presented in separate reports. Their findings to date will be summarized here, however, to help clarify our current understanding of the axial power shape problem.

1. Given an observed critical rod configuration, the GRIMHX calculation of axial power shape frequently will not agree with the observed axial power shape. Because the computed axial power shapes are in error, computed differential rod worths are subject to errors. The latter is a crucial fact because inferred reactivity worths for temperature and fission product changes are derived from computed rod worth curves.
2. Studies performed by APG indicate that the cause of the disagreement above is not due to a deficiency in GRIMHX itself. GRIMHX results were compared against results computed using the industry-standard codes MCNP (continuous energy Monte Carlo) and DIF3D (fine mesh finite difference diffusion theory). In addition, the Physics Methods team wrote a code to generate radially collapsed axial cross sections for use in a 1-D axial S_n code (collapsing was done using the radial flux computed by GRIMHX). There was an acceptable level of agreement between axial flux shapes and differential rod worths computed by the different codes.



Consequently, there does not appear to be any deficiencies with the numerical models in GRIMHX.

3. Analysis has shown that axial depletion effects are not the cause of the discrepancy. Because GRIMHX does not have a burnup capability, simplifying assumptions were made when the differential control rod worths were computed. In those calculations, no axial burnup (or fission product build-in) effects were modelled in GRIMHX. Differences between the calculated and observed flux shapes can not be attributed to this simplification.

4. There are indications that there is a greater variation in core materials at the ends of the target and fuel tubes than previously assumed. This tailing-off or feathering of fuel and target materials outside the center 10 foot section of the tube is commonly referred to as the "end effect." Investigation of this area is still continuing.

5. Finally, if the partial length control rods are adjusted to force agreement between GRIMHX-computed and the observed axial flux shapes, substantial improvement in GRIMHX's predictions of differential rod worths is obtained.

I. INITIAL CRITICAL

Three initial critical positions were found during the first phase of the startup testing program, corresponding to double partial rods at 700, 800, and 950 veeder units. The corresponding full rod positions were 2573, 2285, and 2538 veeder units, respectively. This data is excellent for comparison purposes since the reactor was in the zero power stage throughout this part of the test period, and thus fission product and temperature effects were negligible.

GRIMHX modeling of the three different critical positions resulted in widely different values for k-effective: 0.9850, 0.9804, and 0.9781, for partials at 700, 800 and 950 veeder units, respectively. Note that these values are spread over 700 pcm, or 0.7% Δk . Since axial flux shape is a known concern in the GRIMHX model, a parametric study



was performed by maintaining the same full rod insertion but varying the partial rod position from -40 to +40 veeder units from the actual position in 10 veeder unit increments. The results of this study are shown in Figure 1. To find the point where the maximum difference between the predicted k -effective for the three critical positions is a minimum, a spreadsheet was developed to find the maximum of the difference between k_1 and k_2 , k_2 and k_3 , and k_1 and k_3 . The smallest of these values is where the data come closest to converging. A displacement of +36 veeder units was found to result in the minimum difference between the three values of k -effective: 136 pcm. This shows that GRIMHX-produced axial shapes are too bottom heavy, but can be corrected by adding a bias to the partial rod insertion. This issue will be further discussed in the following sections.

II. PARTIAL ROD INSERTION TEST

Before any attempt was made to improve the GRIMHX model, a direct comparison of GRIMHX and RMS reported axial power shapes was made. This comparison is shown in Figure 2; the axial power shape corresponds to that reported by the APM rods in the reactor just before initiation of the RSP 90-007-12 test (0000 hours on 6/28/92). Since all full and partial control rods were at the same insertion limits, the axial flux shape is relatively uniform across the core; therefore, a reactor averaged axial flux shape was used in these comparisons. Note that the GRIMHX power shape is much more bottom heavy than that reported in RMS. This result explains why GRIMHX predicted a negative reactivity addition: GRIMHX predicted that the test would result in partial rods being inserted into a higher worth region, thus decreasing reactivity. The actual shape is much more flattened than the one predicted by GRIMHX.

A search was performed to find a partial rod insertion position that would result in an axial power shape close to the one reported in RMS. Using this shape as a starting point, it would then be possible to simulate the gang partial rod addition test and predict a positive reactivity insertion. The required partial rod insertion was found by



trial and error, keeping all gang partials at the same level, while leaving the full rods at 1537 veeder units. It was noted during the trial and error procedure that the axial shape was extremely sensitive to small gang partial rod moves. With gang 1 partials at 800 veeder units, the predicted power shape is bottom heavy, at 815 veeder units it is flat, and at 820 veeder units it is top heavy. The closest match (found by visual inspection) occurred when the gang 1 partials were at 815 veeder units; a comparison of the RMS and GRIMHX predicted axial power shapes is shown in Figure 3. Moving the gang 1 partials from 815 to 865 veeder units resulted in a positive reactivity addition of 47 pcm. This indicates that GRIMHX may be able to predict the correct direction of reactivity change if the starting axial power shape is corrected to agree with that observed in the reactor.

Burnup Model and Methodology

Since GRIMHX does not have a 3-D burnup capability and is thus not capable of predicting axial and radial exposure profiles, it was decided to use the Reactor Monitoring System (RMS) data to reconstruct the shapes reported by reactor instrumentation. A computer code was written to access the RMS data banks and obtain the 20 layer axial power shape[†] information at each time for which data was available between the beginning and ending times requested (The authors would like to thank J.J. Taylor for writing the RMS data acquisition interface for this code). The code then performs an exposure averaging of the axial data as shown below:

$$R_{i,j} = \frac{\sum_{k=1}^N R_{i,j,k} (E_k - E_{k-1})}{\sum_{k=1}^N (E_k - E_{k-1})} \quad (1)$$

[†] Each APM rod has 7 sensors, each located at a different axial elevation. The control computer fits this data to obtain a 20 layer shape. Both the raw data and the 20 layer shape are sent during an RMS transfer, but until recently only the 20 layer data was saved. Thus the only choice was to use the 20 layer data.



where $R_{i,j,k}$ is the relative power at layer j for rod i at time k , and E_k is the reactor exposure at time k . $R_{i,j}$ is then the exposure averaged axial power in layer j , rod i . In the APM AVG program, separate values of the exposure sum in the denominator of Eq. 1 are found for each APM rod (since at some exposures no readings were obtained for certain rods). The exposure-averaged axial power shapes for 8 APM rods are plotted in Figure 4 (no readings were available for APM rod 1). The exposure-averaged readings from the 8 APM rods were then averaged to get a single exposure-averaged reactor-averaged power shape. This shape was broken into four regimes and a linear or quadratic curve was fit to the data in each regime, as follows:

| | |
|---|----------------------------|
| $P(z) = -0.64856 + 0.011538z$ | $59.36 \leq z < 148.30$ |
| $P(z) = -0.13711 + 0.011216z - 2.2037 \times 10^{-5} z^2$ | $148.30 \leq z < 319.80$ |
| $P(z) = -14.0740 + 0.092448z - 1.3977 \times 10^{-4} z^2$ | $319.80 \leq z < 357.90$ |
| $P(z) = 5.3134 - 0.011665z$ | $357.9 \leq z \leq 440.36$ |

Based on observations of the power shape, the active core was divided into 7 axial levels, and the fitted equations integrated over each level to find the average relative power, \bar{P} , and the fraction of the total power present in each level, P_{fract} :

$$\bar{P} = \frac{\int_a^b P(z) dz}{\int_a^b dz}$$

$$P_{fract} = \frac{\int_a^b P(z) dz}{\int_A^B P(z) dz}$$

where a and b are the endpoints of the layer of interest, and A and B are the elevations of the bottom and top of the Mark 22 fuel,



respectively. The results of these calculations are shown in Table 1 and in Figure 5.

Assembly powers were obtained from the RMS and averaged over each gang; the results are shown in Table 2a. Since the resulting gang 1 and 2 average assembly powers were very similar, the decision was made to use one value for these two gangs. The radial region containing gangs 1 and 2 is referred to as gang 1/2 in the remainder of this report. Using the exposure-averaged axial power shape given in Table 1, a spreadsheet was used to calculate the axial powers for the three radial regions (gang 1/2, gang 3, and the buckle zone) corresponding to reactor powers of 79 and 116 MW. The results are shown in Tables 2b and 2c. These powers were required for the GLASS depletion problems used to generate axial macroscopic cross sections.

The history of the reactor when RSP 90-007-12 was performed is shown in Figure 6. A series of GLASS (Ref. 3) depletion calculations was executed to model the reactor state just before the start of the gang 1 partial rod insertion test. The first GLASS calculation executed corresponded to the 9 hour period when reactor power was 79 MW (note that the effect of the 3 hours at 21 MW was assumed to be negligible), while the subsequent depletion step corresponded to the 42 hour period that reactor power was approximately 116 MW. The resulting cross sections were correlated by gang as a function of assembly power using a second order polynomial fit. Figure 7 shows the final macroscopic thermal capture cross section for gang 1/2, gang 3 and buckle zone Mark 22's as a function of assembly power. The correlations were used to determine the fewgroup cross sections for the powers listed in Tables 2b and 2c. Correlating cross sections reduced the number of GLASS depletion calculations from 42 to 18.

A GRIMHX model was set up using GRISSET (Ref. 4) to utilize the axially dependent cross sections. Seven unique axial layers were used in this work. GRIMHX jobs were run with and without the 7 layer burnup model, with the gang 1 partial rods at 800 and 850



veeder units. The axial geometry used for the burnup case with gang 1 partial rods at 850 veeder units is shown in Figure 8.

Analysis

Even before the GRIMHX 7 layer model was run, it was anticipated that it would not provide the answer to the axial power shape problem - in fact it would probably make it worse. This is because the exposure-averaged axial power shape used to produce the 7 layer cross sections was slightly top heavy. This resulted in more xenon being built into the top part of the core, resulting in a GRIMHX power shape that was even more bottom heavy than before. Execution of the 7 layer GRIMHX cases confirmed this prediction. The reactivity addition computed with the 7 layer model is slightly more negative than that computed with no depletion effects (-48 pcm versus -36 pcm). A comparison of the axial power shapes before the partial rod move for the 7 layer burnup model and the standard GRIMHX (no depletion modeling) is shown in Figure 9. The conclusion is that while the inaccurate reactivity worth prediction is due to an incorrect axial flux shape in GRIMHX, this shape is not caused by axial xenon build-in.

The full length control rod position before initiation of the partial rod move test was 1536 veeder units. During the test, full rods were moved to compensate for the reactivity change caused by the partial rods. When the gang 1 partials arrived at 850 veeder units, the full rods were inserted to 1576 veeder units. Since the reactor was critical at both states, the values of k-effective calculated by GRIMHX should be identical. A series of GRIMHX jobs were run with the full rods fixed at these two positions, while the partial rods were displaced from their nominal positions by 0 to 50 veeder units in 5 veeder unit increments. The results are shown in Figure 10. Note that with no displacement, the values of k-effective differ by 108 pcm, while they are identical at a partial rod displacement of +19 veeder units.



II. XENON WORTH CALCULATIONS

In this section, xenon worth predictions are compared to "observed" xenon worths at the time immediately preceding initiation of the RSP 90-007-12 test, specifically, at 0000 hours on 6/28/92.

Observed Xenon Worth

Observed xenon worth associated with a rise in power is found by comparing control rod worth before the power increase to control rod worth some time after achieving the new power. The case analyzed here is the power ascension from 79 MW to 116 MW, which began at 0500 hours on 6/26 (referred to as "beginning" from here on).

Control rod positions at 79 MW were 2223 veeder units, both partials at 800 veeder units, in all gangs. Forty two hours later (6/28 at 0000 hours), just before initiation of RSP 90-007-12, control rod positions were 1537 veeder units, both partials at 800 veeder units, in all gangs (this time is referred to as "ending" from here on).

Standard GRIMHX calculations using cold-clean beginning-of-cycle cross sections showed a reactivity difference of 782 pcm between the beginning and ending states. In order to account for the differing amounts of xenon present at the beginning and ending reactor states, the 7 layer model described in Section 1 was used to find the worth of the full length control rods with the appropriate amounts of xenon built in at each state. These worths were 3710 pcm (6/26 at 0500 hours) and 2923 pcm (6/28 at 0000 hours). The difference between these values gives a worth for the rod move of 787 pcm, which indicates xenon concentration was low enough that it did not affect the rod worths.

Predicted Xenon Worths

Several tools have been used to predict xenon worth for comparison to the observed values. The XCP22 (Ref. 5) code was developed by



Reactor Engineering for just this purpose; it predicts a differential xenon worth between the two states of 513 pcm. XCP22 calculations are based on GLASS-generated libraries; therefore, it was decided to execute a series of GLASS calculations to verify the XCP22 results. The GLASS calculations were performed executing GLASS depletion problems corresponding to 9 hours at a power of 79 MW followed by 42 hours at 116 MW. Xenon concentrations were recorded from the GLASS edits, and then used in GLASS static calculations to determine the xenon worth as a function of time (the control tube Li6 content remained constant during all of these static calculations, so that any change in k-effective was due solely to the changing xenon concentration). Figure 11 plots the xenon concentration versus time while Figure 12 shows the xenon reactivity worth versus time. The final xenon worth after a total of 51 hours of reactor operation at power was found to be 507 pcm. Exact agreement with XCP22 was not expected since that code accounts for radial power shape by using gang statistical weights. However, the agreement between the two calculations is very close and does verify the XCP22 result.

Analysis

Since the predicted xenon worth (513 pcm) is only 65% of the "observed" worth (787 pcm), one of the two values has not been correctly evaluated. It is important to note that the "observed" value is, in fact, a value inferred from the observed control rod positions and relies on the ability of GRIMHX to accurately predict control rod worth. In an attempt to resolve this issue, a different approach was taken to the problem. Since the reactor was in a stable, critical state both before and after the rise in power from 79 MW to 116 MW, the total reactivity change resulting from the combination of control rod withdrawal and xenon build-in should equal zero, or:

$$\Delta k_{\text{total}} = \Delta k_{\text{rods}} + \Delta k_{\text{Xe}} = 0$$

Modeling of the two reactor states using the 7 axial layer fuel model to account for the differing amounts of xenon at each state resulted



in a total reactivity change of 222 pcm (the k -effective for the two states should have been identical, resulting in a zero reactivity change). Since axial flux and power shape predictions have shown some discrepancies with observations, it was decided to move all partial rods uniformly at the beginning and ending states to see if a $\Delta k_{total} = 0$ could be achieved. Figure 13 shows the variation of k -effective versus partial rod position for both the beginning and ending states. The two curves intersect at a partial rod insertion of approximately 835 veeder units. At this point, $\Delta k_{total} \approx 0$, so $\Delta k_{xenon} \approx -\Delta k_{rods}$. The rod worths were re-calculated at each state with all partial rods at 835 veeder units: the new worths are 4256 pcm (beginning) and 3672 pcm (end). The resulting worth for the rod move from 2223 veeder units to 1537 veeder units is -584 pcm, which indicates a xenon reactivity worth of +584 pcm. This value was independently verified by performing GRIMHX calculations with and without xenon at the beginning and end states. Subtracting the total xenon worth at the beginning state from that at the end state then gives the differential xenon worth associated with the increase in power. This value was -573 pcm, which is in good agreement with the value inferred from the rod worth. Therefore, with the partial rods adjusted such that k -effective between the beginning and ending states is the same (as it should be), the xenon worth predicted by GRIMHX is approximately -580 pcm. This value is much closer to the XCP22 and GLASS predictions (approximately 510 pcm) than the 782 pcm previously assumed. The remaining discrepancy (13%) between the results may be due to the fact XCP22 and GLASS results are based on 2-D infinite lattice calculations that do not account for axial flux shapes.

This analysis further demonstrates GRIMHX deficiencies in axial flux shape prediction and also shows that inferring xenon worth from current rod worth curves may not be accurate. On the other hand, the accuracy of GRIMHX reactivity predictions is greatly improved when adjustments are made to correct the axial flux shape.



CONCLUSIONS

The analyses reported in this paper clearly demonstrates that GRIMHX-produced axial power shapes are too bottom heavy. Two totally independent analyses (initial critical and xenon reactivity worth) resulted in an optimum partial rod bias of +36 veeder units, while the gang 1 partial rod move test was best resolved with a partial rod bias of +19 veeder units.

A large volume of data remains to be analyzed. Gang partial rod move tests were performed for all three gangs at three different partial rod insertion levels; only 1 of these nine tests was simulated in this work. Over 20 different power ascensions were made during the test period; many of these are suitable for xenon reactivity analysis. In addition, no attempt to model temperature reactivity effects using the 7 layer model has yet been made. Finally, a large number of critical positions were measured at zero power; only three were analyzed here. Analysis of this data using the methodology presented in this paper would be prohibitively time consuming unless some of the data preparation steps can be automated. The APMAVG code is currently being modified to perform all the necessary calculations such that layer powers for each gang are output for a specified reactor operation time period. In addition, a driver module is being written to repeatedly execute GLASS and produce the necessary fewgroup cross sections. This work will be reported in a later document.



REFERENCES

1. D.G. Erikson, R.D. Crowe, and E.F. Trumble, *GRIMHX User's Manual (U)*, WSRC-TR-91-354, September 1991.
2. S.K. Andre *et al*, *Axial Power Monitor Rod Issues and Resolution for K-14.1*, WSRC-RP-92-594, May 1992.
3. R.L. Frost and S.H. Finfrock, *GLASS User's Manual (U)*, WSRC-TR-91-143, January 1992.
4. J.J. Taylor, G.R. Cefus, and R.L. Webb, *GRISSET User's Manual, Revision 1 (U)*, WSRC-TR-92-85, February 1992.
5. Deborah J. Henrikson, *XCP22 User and Programmer Manual (U)*, WSRC-TR-91-42-015, April 26, 1991.



TABLE 1.

Average Relative Power and Axial Level Designations

| Axial Level | Elevation (cm) | Average Relative Power | Percent of Power (%) |
|-------------|-----------------|------------------------|----------------------|
| 1 | 59.36 - 100.00 | .271 | 3.07 |
| 2 | 100.00 - 125.00 | .649 | 4.53 |
| 3 | 125.00 - 148.30 | .928 | 6.03 |
| 4 | 148.30 - 319.80 | 1.227 | 58.66 |
| 5 | 319.80 - 357.90 | 1.187 | 12.61 |
| 6 | 357.90 - 400.00 | .893 | 10.48 |
| 7 | 400.00 - 440.36 | .412 | 4.64 |



TABLE 2a.

Average Assembly Powers by Gang

| Gang | Reactor Power of 116 MW | Reactor Power of 79 MW |
|------|-------------------------|------------------------|
| 1/2 | 0.3055 | 0.1968 |
| 3 | 0.2497 | 0.1609 |
| 4 | 0.2006 | 0.1293 |

TABLE 2b.

Assembly Powers for Reactor Power of 79 MW¹

| Axial Level | Power Fraction | Gang 1 & 2 (MW/ft) | Gang 3 (MW/ft) | Gang 4 (MW/ft) |
|-------------|----------------|--------------------|----------------|----------------|
| 1 | 0.0307 | 0.0045 | 0.0037 | 0.0030 |
| 2 | 0.0453 | 0.0109 | 0.0089 | 0.0071 |
| 3 | 0.0603 | 0.0155 | 0.0127 | 0.0102 |
| 4 | 0.5866 | 0.0205 | 0.0168 | 0.0135 |
| 5 | 0.1261 | 0.0199 | 0.0162 | 0.0130 |
| 6 | 0.1048 | 0.0149 | 0.0122 | 0.0098 |
| 7 | 0.0464 | 0.0069 | 0.0056 | 0.0045 |

TABLE 2c.

Assembly Powers for Reactor Power of 116 MW²

| Axial Level | Power Fraction | Gang 1 & 2 (MW/ft) | Gang 3 (MW/ft) | Gang 4 (MW/ft) |
|-------------|----------------|--------------------|----------------|----------------|
| 1 | 0.0307 | 0.0070 | 0.0057 | 0.0046 |
| 2 | 0.0453 | 0.0169 | 0.0138 | 0.0111 |
| 3 | 0.0603 | 0.0241 | 0.0197 | 0.0158 |
| 4 | 0.5866 | 0.0318 | 0.0260 | 0.0209 |
| 5 | 0.1261 | 0.0308 | 0.0252 | 0.0202 |
| 6 | 0.1048 | 0.0232 | 0.0190 | 0.0152 |
| 7 | 0.0464 | 0.0107 | 0.0087 | 0.0070 |

¹Exposures determined based on listed gang power and 9 hour depletion time.

²Exposures determined based on listed gang power and 42 hour depletion time.

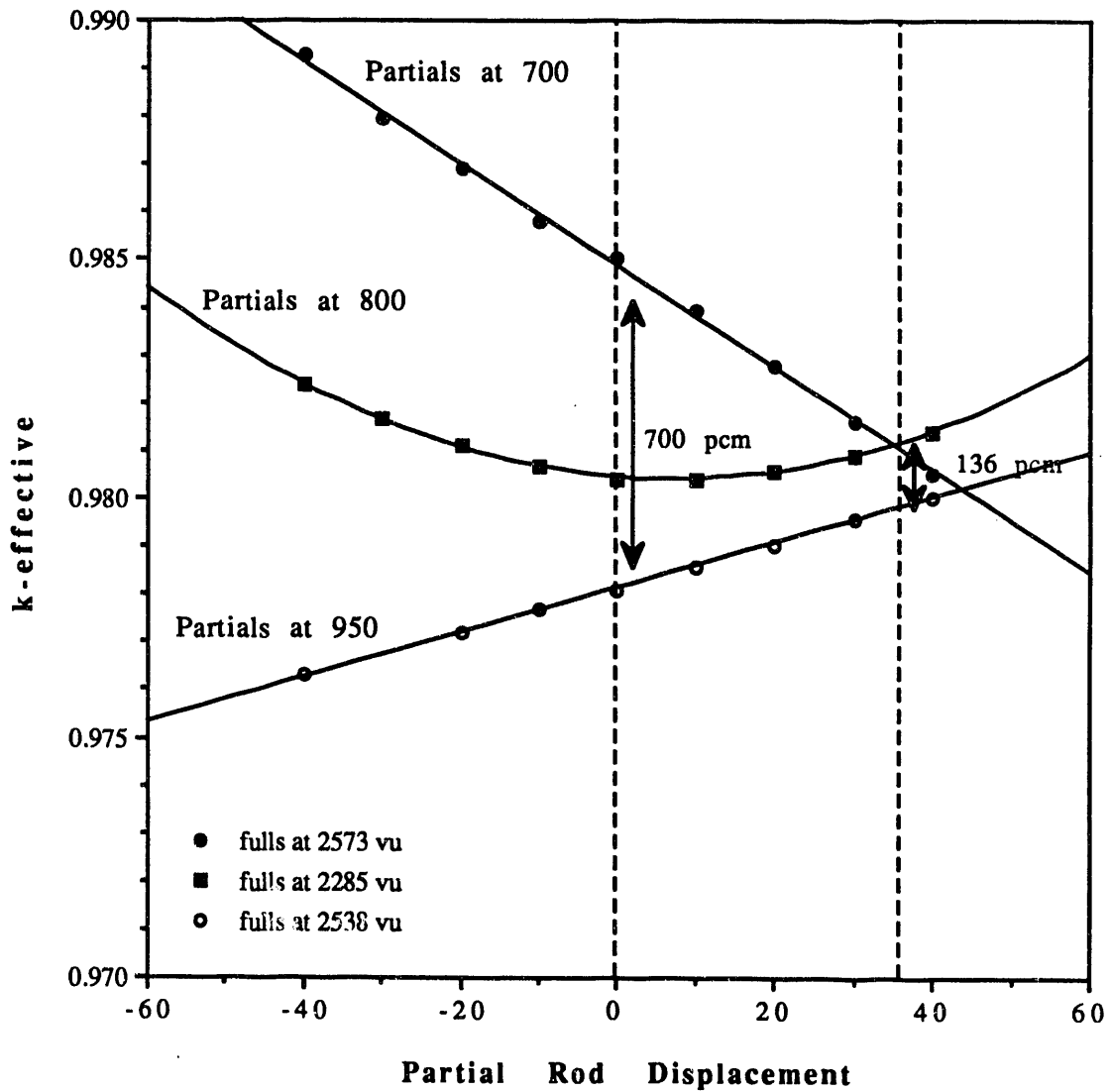


Figure 1. K -effective versus partial rod displacement with full rods at the three initial critical values. The difference in k -effective for the three curves is smallest at a displacement of approximately 36 weeder units.

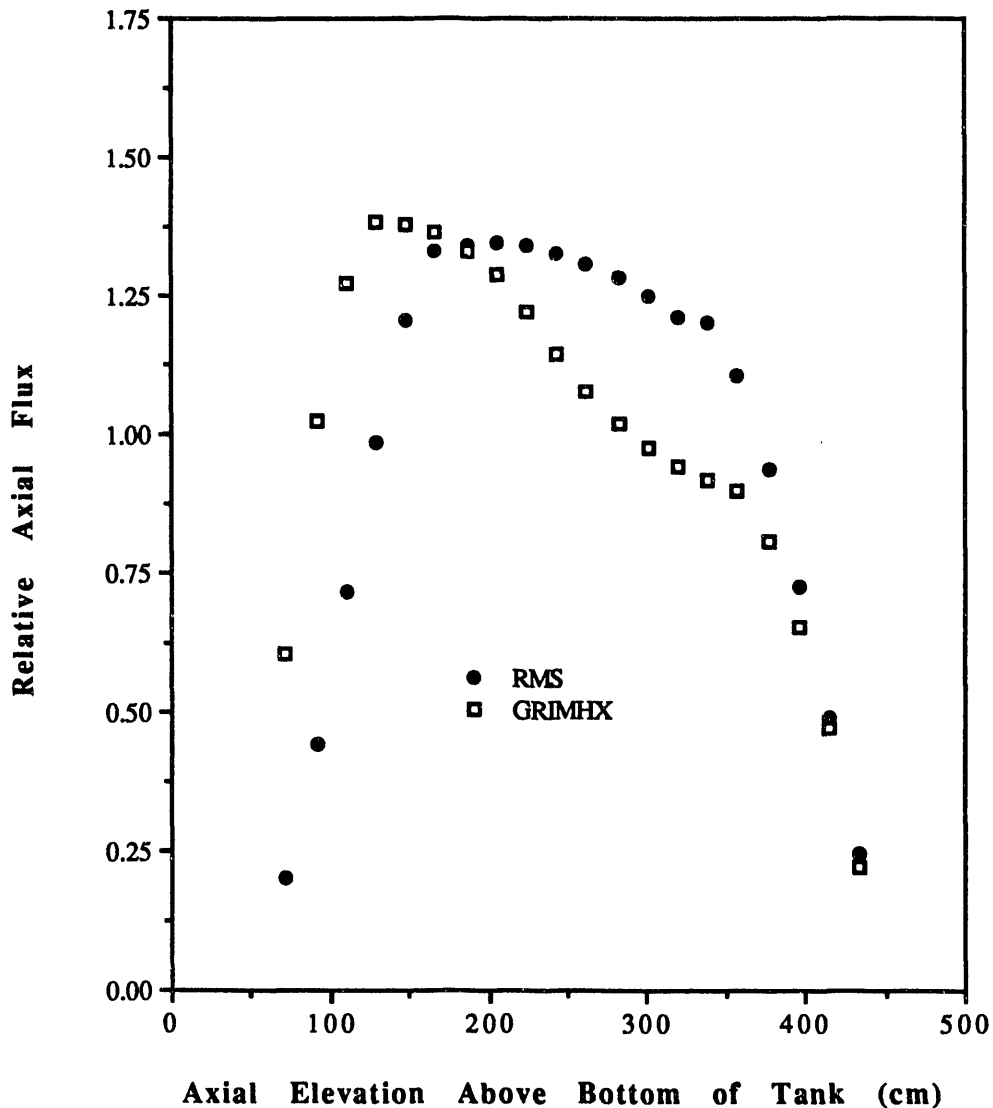


Figure 2. Comparison of GRIMHX and RMS axial power shapes. This is a snapshot view immediately preceding the gang 1 partial rod move (6/28 at 0000 hours). Each graph represents the average of the readings from the 9 APM rods (in GRIMHX, the predicted axial power shape at each APM rod position is determined using the XGRIM3D code).



GRIMHX Predictions of Axial Power Shapes and Xenon Worth with 3-D Depletion Modeling

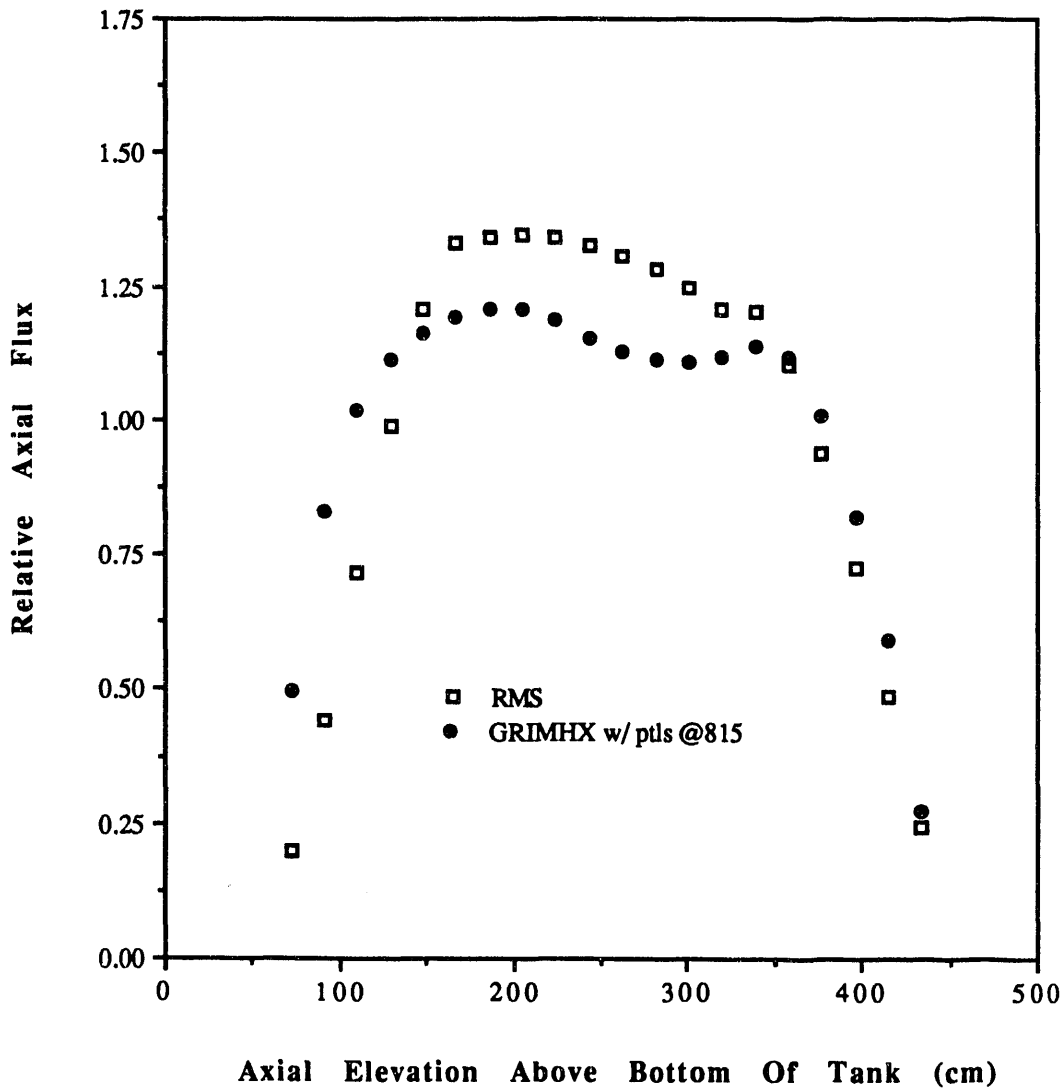


Figure 3. Comparison of the reactor-averaged axial power shape at a time just prior to the gang 1 partial rod move (6/28 at 0000 hours). The GRIMHX shape was produced with all partials at 815 veeder units.

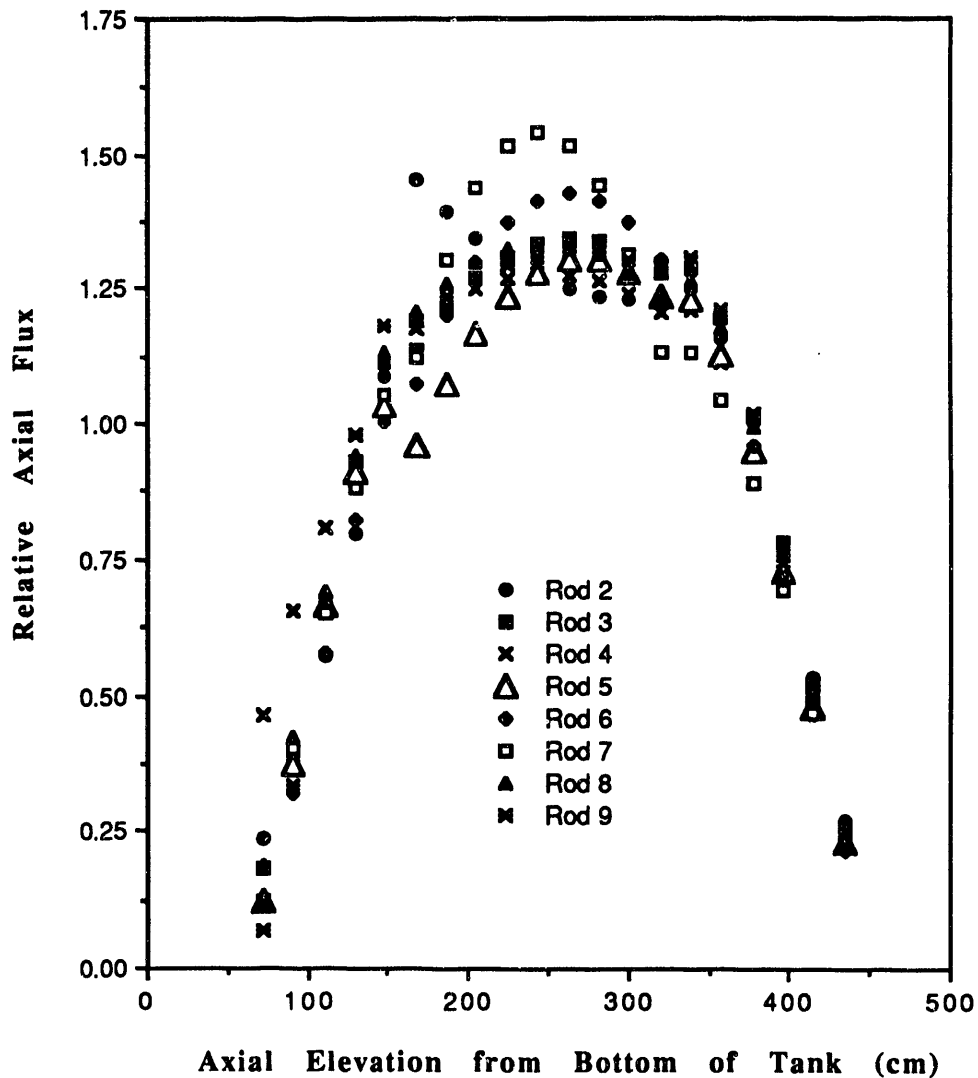


Figure 4. Exposure averaged (6/25-6/28) axial power shapes for APM rods 2-9 (no data was available for APM #1).

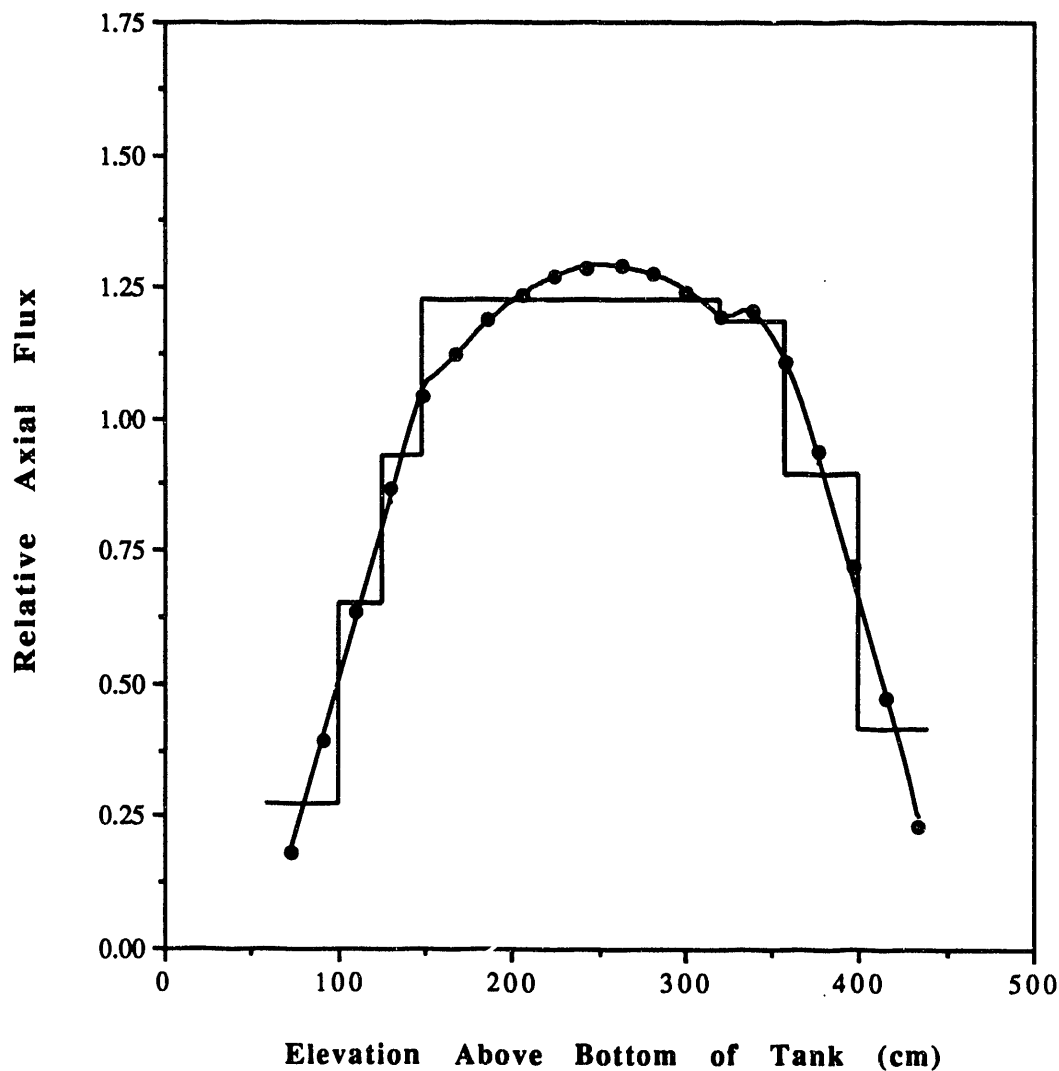


Figure 5. The solid circles show the exposure-averaged (6/25 through 6/28), reactor-averaged axial power shape. The line through the circles is the result of the composite curve-fitting. The histogram shows the calculated average power in each of the 7 axial levels used in the modeling.

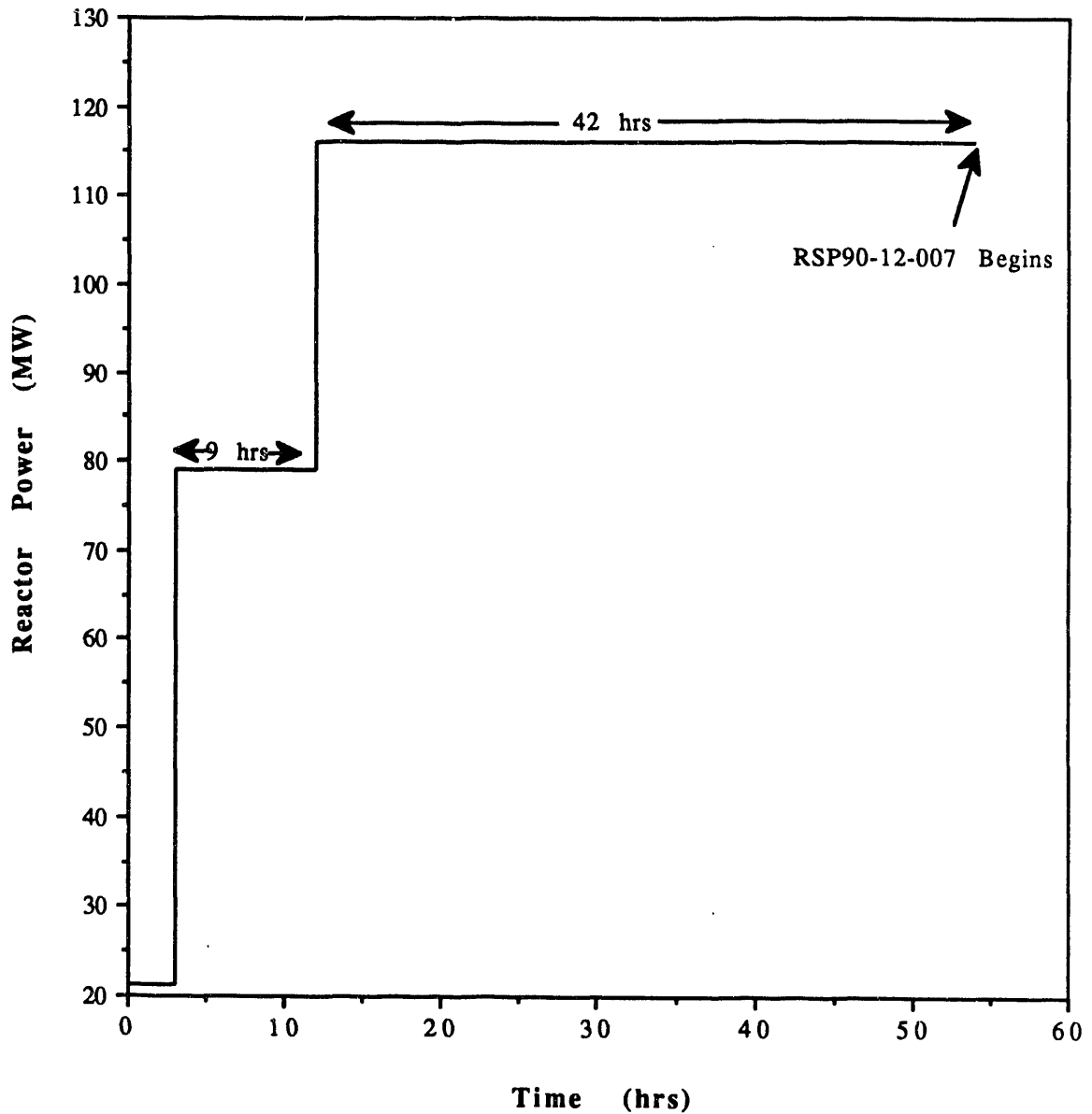


Figure 6. Power history of K-reactor, starting at 1700 hours on 6/25/92.

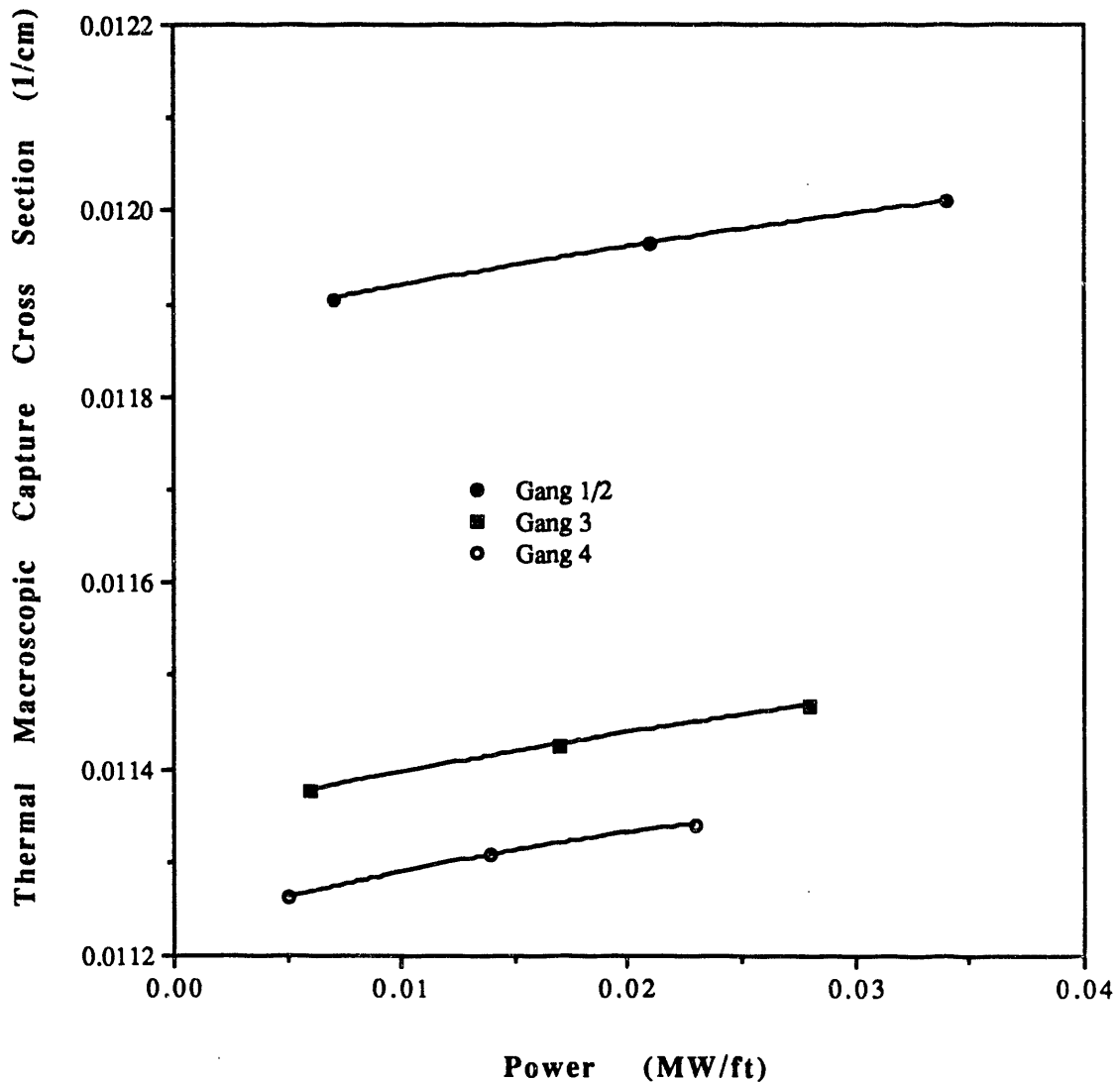


Figure 7. Thermal macroscopic cross section as a function of assembly power. Note that here power is directly proportional to exposure. All depletion problems were run for the same amount of irradiation time, and exposure equals power multiplied by the time at that power. The powers for which the data is plotted correspond to the appropriate ranges in Table 2c.



GRIMHX Predictions of Axial Power Shapes and Xenon Worth with 3-D Depletion Modeling

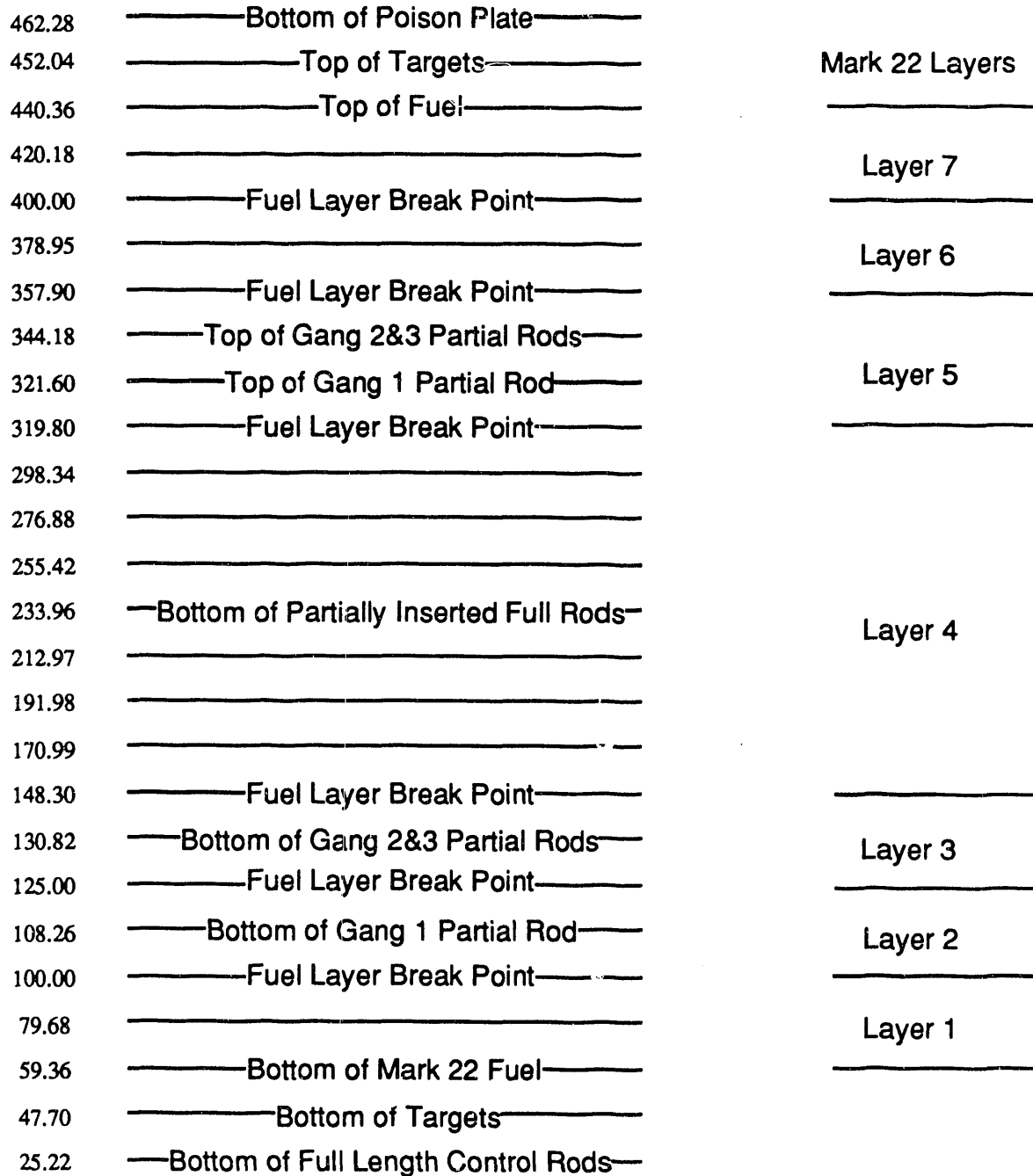


Figure 8. Axial elevations used in GRIMHX model.

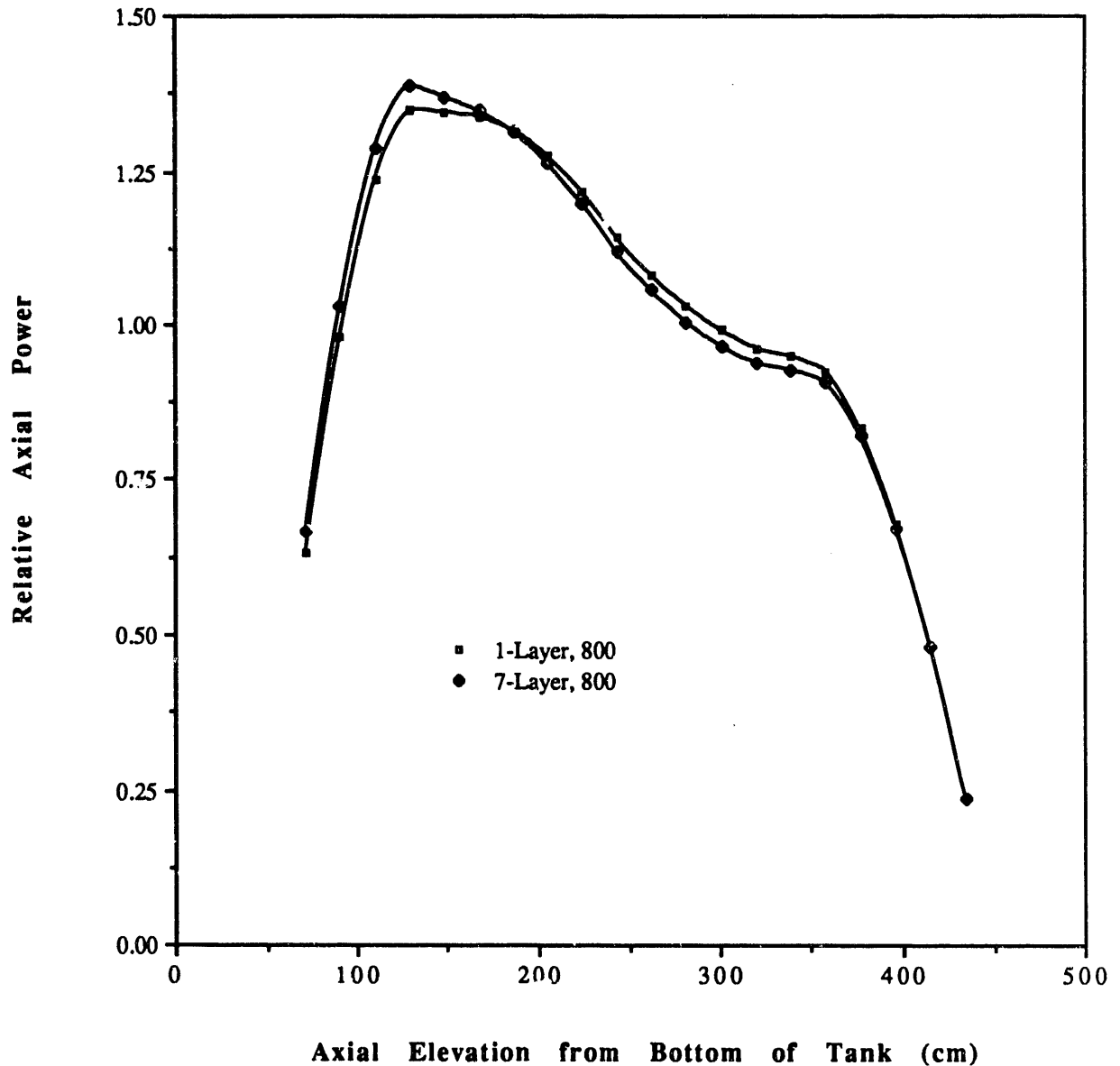


Figure 9. Comparison of the axial power shapes computed by GRIMHX with and without the axial depletion modeling (6/28 at 0000 hours). The differences are small because the charge has little exposure at this point.

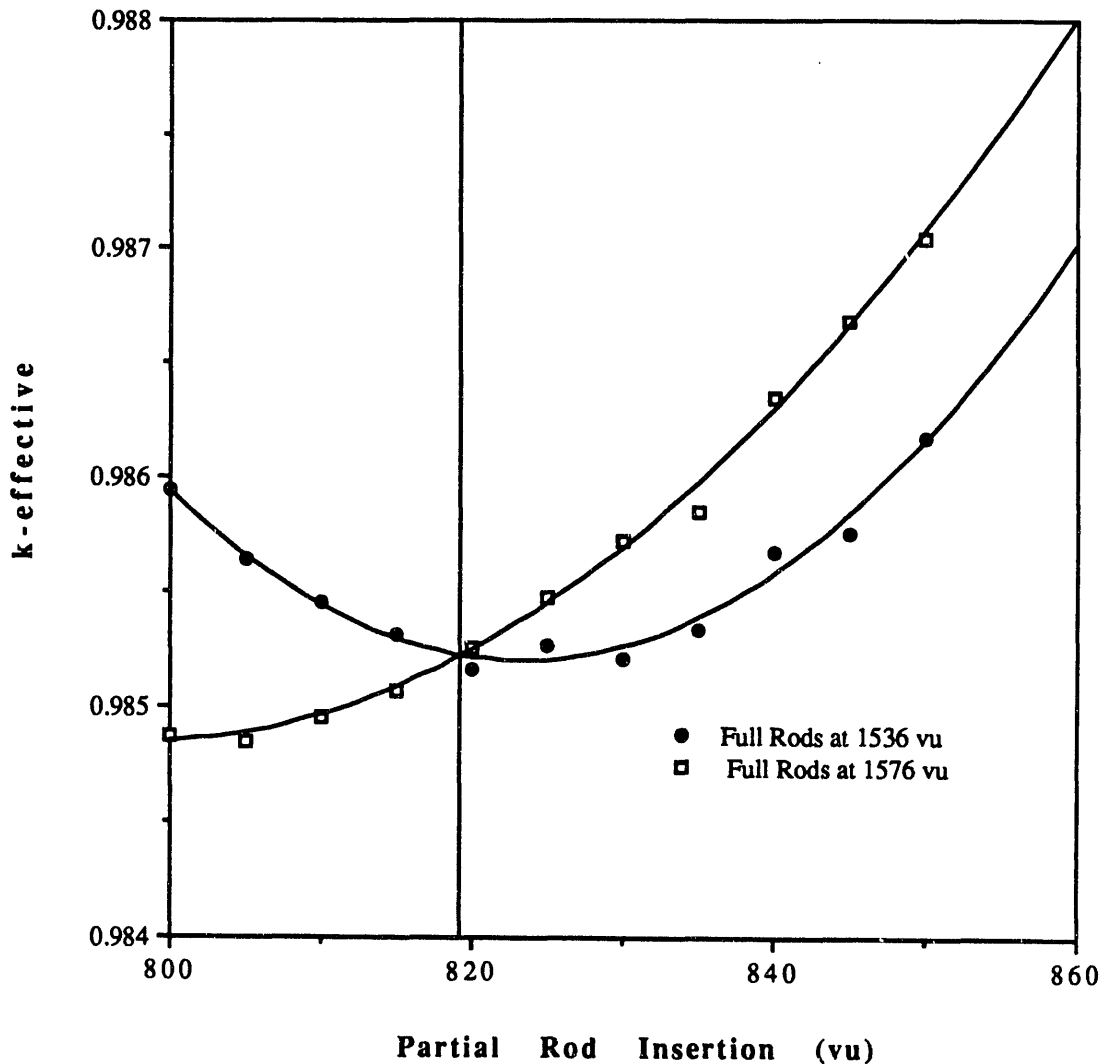


Figure 10. GRIMHX-calculated values of k -effective versus positioning of the double partial rods for the gang 1 partial rod move test. The values of k -effective are equivalent at a partial rod displacement of approximately +19 veeder units.

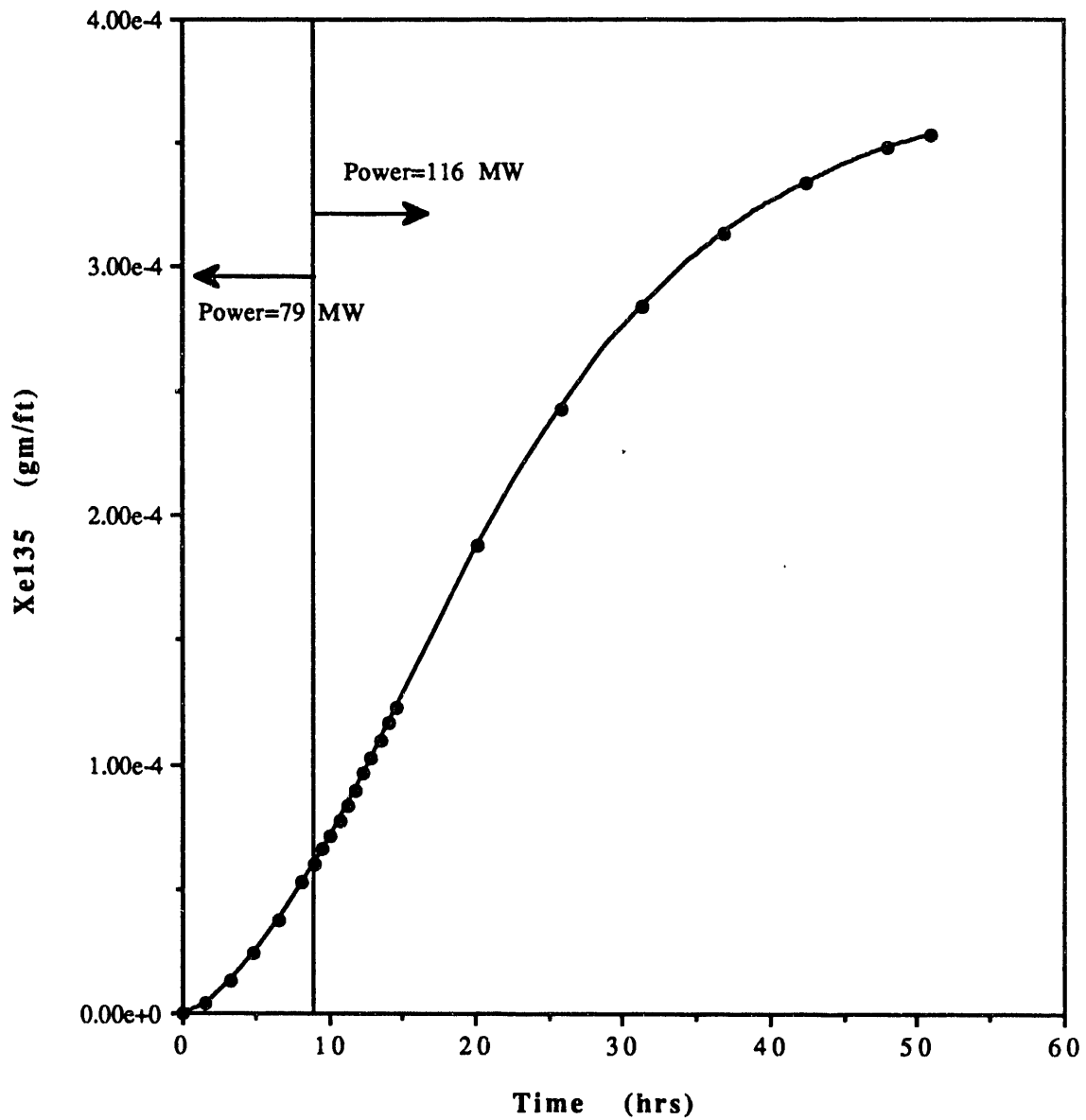


Figure 11. GLASS-generated xenon concentration as a function of time. On this graph, t=0 corresponds to the point where reactor power was first raised to 79 MW (6/25 at 2000 hours), while t=51 hours corresponds to the time when the RSP90-007-12 test was begun (6/28 at 0000 hours).



GRIMHX Predictions of Axial Power Shapes and Xenon Worth with 3-D Depletion Modeling

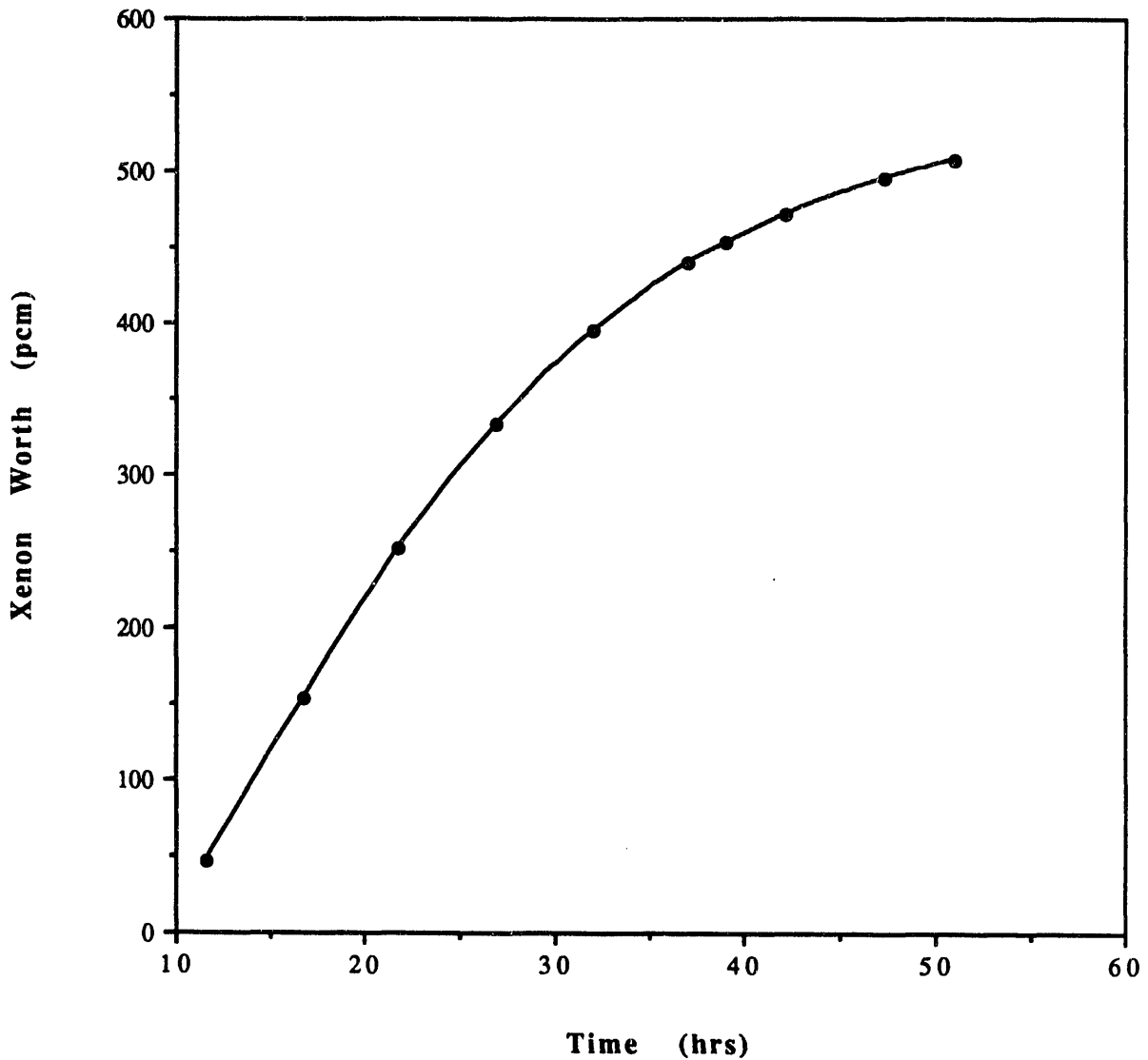


Figure 12. GLASS-generated xenon worth as a function of time. As in Figure 11, $t=0$ corresponds to the point where power was initially raised to 79 MW, while $t=51$ corresponds to the beginning of the RSP90-12-007 test.

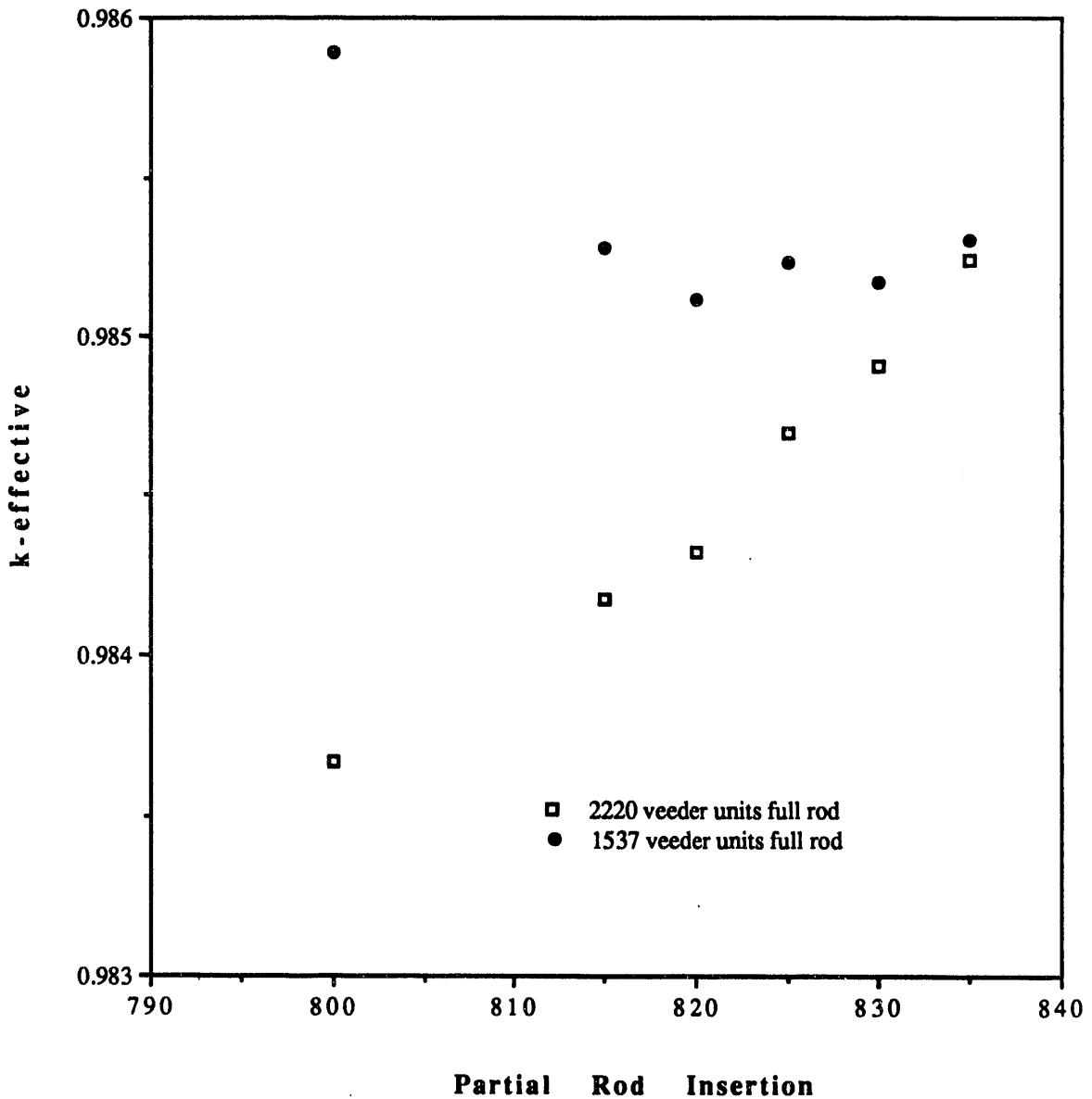


Figure 13. k-effective versus partial rod position. The open squares represent a full rod insertion of 2220 veeder units, with xenon corresponding to 9 hours at 79 MW. The solid circles represent 1537 veeder units of full rod with xenon corresponding to 9 hours at 79 MW followed by 42 hours at 116 MW.

END

**DATE
FILMED**

2 / 22 / 93

